Ceramic nanocomposites: control of structural and PTX parameters of the synthesis of mullite from kaolinite using Taguchi experimental design

A. PONARYADOV ▪ Institute of Geology, FRC Komi Science Center of Ural Branch of RAS, Syktyvkar, Russia ▪ alex401@rambler.ru
O. KOTOVA ▪ Institute of Geology, FRC Komi Science Center of Ural Branch of RAS, Syktyvkar, Russia
E. KOTOVA ▪ St. Petersburg Mining University, St. Petersburg, Russia

Érkezett: 2023. 04. 25. ▪ Received: 25. 04. 2023. ▪ https://doi.org/10.14382/epitoanyag-jsbcm.2023.21

Abstract
The purpose of this article is to develop a special modeling approach, which simulates the synthesis of a mullite from kaolinite and allows controlling its physical and structural properties. A Taguchi experimental design is implemented to reveal significant PTX-parameters in comparison with insignificant ones for the synthesis of a mullite nanocomposite and prototyping of the optimal synthesis protocol.
The objects of the study are ceramic nanocomposites: morphostructural characteristics of mullite synthesized from kaolinite and its structural transformations during heat treatment. 2D contour plots of the intensity of mullite XRD-peaks and content of the mullite phase were used to visualize the influence of input factors and point out the optimal ones. Furthermore, we rearranged the previously proposed simple mathematical model of structural transformations "kaolinite – mullite", which allows controlling the synthesis protocol and properties of the mullite matrix of nanocomposite depending on the PTX-parameters of mullite synthesis.
Keywords: ceramic nanocomposites, mullite, kaolinite, Taguchi method, modeling, PTX-parameters
Kulcsszavak: kerámia nanokompozitok, mullit, kaolinit, Taguchi módszer, modellezés, PTX-paraméterek

Aleksei V. PONARYADOV
is a Researcher of Laboratory of Technology of Mineral Raw, Institute of Geology, Komi Science Center, Ural Branch of the Russian Academy of Sciences. Author and co-author of more than 30 scientific articles. Russian Mineralogical Society.

Olga B. KOTOVA
is professor and Head of Laboratory of Technology of Mineral Raw, Institute of Geology, FRC Komi Science Center, Ural Branch of the Russian Academy of Sciences. Author and co-author of 4 patents and more than 150 scientific articles.Vice-president of International Commission on Applied Mineralogy (IMA-ICAM). Member of Russian Mineralogical Society.

Elena L. KOTOVA
is a Scientific director of the Mining museum of the Saint-Petersburg Mining university. Author and co-author of chapter in book, 1 patent and 32 articles. The member of the Russian Mineralogical Society, Oil and gas historical Society of Russia.

1. Introduction

The synthesis of nanostructured natural-like functional materials based on natural mineral raw materials of various genesis seems to be a difficult task for technologists, which involves many necessary parameters within a unified multi-level system of the production process. The main disadvantage of natural raw materials is the presence of impurities affecting technological processes [1, 2] and quality of the target product [3-5]. Kaolin is known to be "the cleanest" clay from various "harmful" impurities for the production of ceramic nanocomposites. The use of these clays as a raw material is significantly reduced by the cost of production [6-8].

Mullite ceramics are multifunctional material, characterized by a high strength and a chemical stability in aggressive environments, which is widely used in various directions of industry, including high-temperature technological processes [9-11].

Mullite is formed from kaolin clay during heat treatment as a result of an exothermic reaction occurring in the interval of 1200–1400 °C (the solid-phase synthesis), which makes this process extremely energy-consuming [6, 12]. The temperatures at which the polymorphic transformations of the samples occur are explained by features of their chemical and phase compositions (including impurities [13, 14]), parameters of synthesis (heating rate [15]), structural features, for example, the presence of voids in mullite crystal lattice up to 0.067 nm leads to the formation of solid solutions with various oxides (Fe_2O_3, TiO_2, CaO, etc.), which also affects both technological properties of composites and synthesis protocol [16]. Thus, the synthesis of nanocomposites based on mineral raw materials of various genesis is a comprehensive task requiring the assessment of many parameters, which, within the framework of production, must be tied into a unified multi-level system.

Currently, the global trends and technological challenges, including the production of high-tech ceramics and nanocomposites, make the search for new approaches to assessing the purity and composition of raw materials [17, 18] and modeling the physicochemical properties of target prototypes for industrial applications [19-21] very relevant.

The use of mathematical approaches to calculating consistency of the relationship between the structure and properties of mineral raw materials for innovative environmentally friendly technologies for processing and operation, as well as to create ceramic composites with specified properties, can significantly reduce labor costs [22, 23]. In addition to the "classic" methods for calculating the kinetic constants of the reaction of the formation of mullite [24] and the assessment of thermodynamics of the process, mathematical modeling is used [25].

The mathematical modeling of mullite synthesis makes it possible to single out significant parameters in comparison with insignificant ones, simplifying the procedure for the synthesis of materials with specified characteristics. Design of experiments (e.g. Taguchi method, response surface methodology) is a powerful tool to simplify a huge number

of variables and minimize number of experiments for obtaining the optimum synthesis protocol. All parameters are systematically investigated as well as their interactions which made the acquired information more reasonable than results of influence of a separate factor. A key-feature of the Taguchi method is its versatility – applicability in various fields (electronics [26], biotechnology [27, 28], etc.) and a reduction in the number of experiments on finding optimal combination of parameters in the quality engineering [29, 30].

The aim of the study is to develop the near-to optimal synthesis protocol of a mullite nanocomposite from kaolinite with control of physical and structural properties of target product using Taguchi experimental design approach.

2. Methods and approaches

Solid-phase synthesis. Samples of kaolin clay (Vezhayu-Vorykvinsky deposit, Russia, the content of kaolinite >98%, the chemical composition is given in *Table 1*) were grinded in the laboratory disk grinder LDI-65. The load of 1.5–1.6 g was additionally grinded in the agate mortar and using the standard set of sieves was divided into fractions +0.1, –0.1+0.071, –0.071+0.05, –0.05 mm. As an introduced agent-crystallizer ("impurity"), mullite was used, which was previously synthesized according to the method [8], in the amount of 0.5, 1 and 5 wt.%. Heat treatment of samples and prepared mixtures with an agent-crystallizer was carried out at temperatures of 1100, 1150, 1200 °C in the atmosphere inside tube furnace Carbolite Gero TF1 16/60/300, heating rate 5, 10, 20 deg/min, holding time 2 hours at normal atmospheric pressure.

SiO_2	Al_2O_3	TiO_2	Fe_2O_3	K_2O	CaO	MgO
51.41	43.79	1.83	1.53	0.43	0.38	0.33

Table 1. Chemical composition of kaolin clay, wt.%
1. táblázat A kaolin agyag kémiai összetétele, tömegszázalékban

Calculation methods. The phase composition of the samples was determined by XRD-patterns of unoriented samples, X-ray diffractometer Shimadzu XRD-6000, radiation CuKα, Ni-filter, 30 kV, 20 mA, scanning range 2–65° 2θ. The phase content was evaluated by the Rietveld method (Profex software). Morphostructural characteristics of the samples were studied by scanning electron microscopy (SEM Axia ChemiSEM LoVac, Thermo Scientific).

To analyze the results of the experimental data and quality engineering of the resulting mullite nanocomposite, the Taguchi method was used, which is based on the use of Orthogonal Arrays (OA) [26]. As a target parameter, the intensity of mullite peaks on XRD-patterns was used.

To calculate the deviation between the experimental and optimal values of the input parameters, the Signal-to-Noise ratio (S/N) loss function was used. To optimize the synthesis protocol, the type of function "Higher-is-Better" (HB) was selected.

The values of the S/N ratio denoted by η_{ij}, where the i-th characteristic of the evaluated parameter obtained in the j-th experiment will be determined by the following logarithmic ratio:

$$\eta_{ij} = -10log\left(\frac{1}{n}\sum_{i=1}^{n} \frac{1}{I^2}\right) \quad (1)$$

where I stands for the resulting value (the intensity of the peak on the XRD-pattern), and n – the total number of experiments ran in the given experimental conditions.

The influence of experimental parameters ("weight") was determined by the Analysis of Variance (ANOVA) [29], by which instrumental errors in determining the intensities of mullite peaks on XRD-patterns are also evaluated.

3. Results and discussion

XRD, structural transformation of kaolinite. The crystalline structure of kaolinite includes alternating silicon tetrahedron and octahedral alumo-oxygen-hydroxyl layers [31, 32]. With an increase in temperature, as the interlayer water molecules are removed, there is a gradual decrease in the intensity of the reflections of X-ray radiation from the basal planes of kaolinite (peak at 2θ = 24.9°, green curve, *Fig. 1*). In the temperature range of 700–900 °C, the initial sample becomes almost X-ray amorphic (a significantly blurred area of diffuse scattering is preserved, which corresponds to the intermediate phase – metakaolinite). The mullite phase is fixed at temperatures above 1100 °C (peak at 2θ = 40.85°, red curve, *Fig. 1*). The crystalline structure of the mullite consists of paired Si_2O_5 chains, in which silicon ion is partially isomorphically substituted by aluminum ion, which has both the 6-fold [AlO_6] and the 4-fold [AlO_4] coordination [8, 33]. In parallel, cristobalite is formed due to an excess of unrelated silica (in mullite Al/Si = 3, while in the original kaolinite Al/Si = 2).

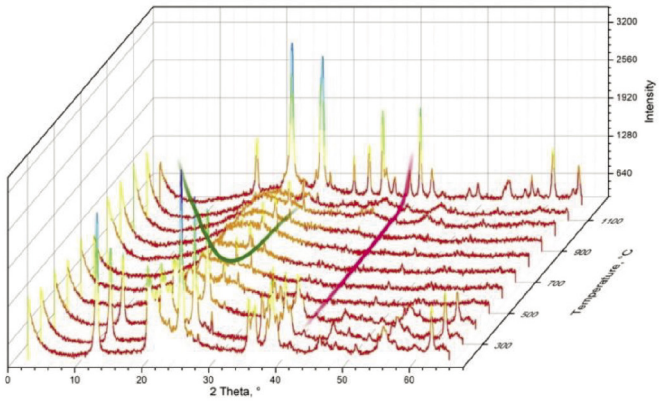

Fig. 1 Structural transformations of kaolinite during heat treatment
1. ábra Hőkezelés során a kaolinit szerkezeti átalakulásai

The morphostructural characteristics of the kaolinite and mullite synthesized at 1200 °C are represented in *Fig. 2*. The kaolin is most often represented by deformed and cemented individuals of kaolinite (*Fig. 2(a)*). Isometric crystals of kaolinite – hexagonal prisms – are rare. During heating, the matrix is recrystallized, which results in the formation of larger individuals of kaolinite. The sample heat treatment at temperatures above 1100 °C leads to the formation of elongated prismatic crystals of pseudomullite (*Fig. 2(b)*). The formation of new mineral phases begins on the surface and gradually spreads throughout the volume of the sample. At the last stages of temperature transformations, the appearance of cristobalite was recorded.

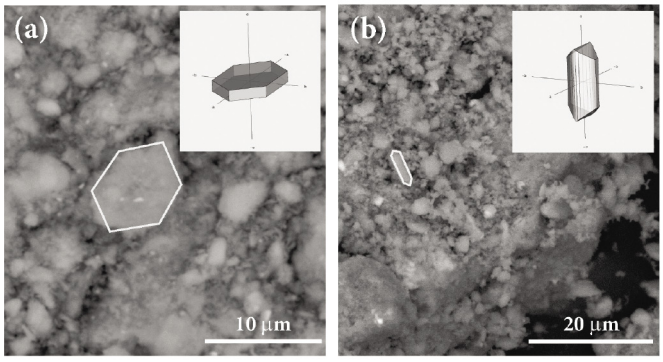

Fig. 2 Morphostructural characteristics of kaolinite (a) and mullite synthesized at 1200 °C (b) (SEM, back-scattered electrons)
2. ábra A kaolinit (a) és az 1200 °C-on szintetizált mullit (b) morfológiai jellemzői (SEM, visszaszórt elektronok)

It was shown [25], that for kaolinite, the intensity of peaks on XRD-patterns (*Fig. 1*) is approximated by linear dependence at temperatures below 450 °C and parabolic at higher temperatures, while for mullite the dependence is exponential: $I(t) = e^{(\pm I_0 \pm \alpha t)}$. The α-coefficient can be rearranged by introducing main parameters that affect the kinetics of the process of mullite synthesis – sample heating rate θ, concentration of the impurities σ, particles size d and k_i – proportionality coefficient, reflecting the "weight" of the influence of the considered parameters:

$$\alpha = \frac{k_1 \sigma}{k_2 \theta \cdot k_3 d} \quad (2)$$

Eq. (2) is a simplified mathematical model of structural transformations in the "kaolinite – mullite" series. However, the considering of the above mentioned synthesis input parameters one will need to run approximately one hundred experiments of mullite nanocomposite synthesis. To minimize number of experiments and clarify the interactions between the variables and obtain the optimum synthesis protocol the Taguchi method was used.

Parameter	1	2	3	4
***d*, particle size, mm**	–0.05	–0.071+0.05	–0.1+0.071	+0.1
***θ*, heating rate, deg/min**	5	10	20	–
***σ*, impurity concentration, wt. %**	0	0.5	1	5
***t*, holding temperature, °C**	1100	1150	1200	–

Table 2 Design parameters of mullite synthesis
2. táblázat A mullit szintézisének tervezési paraméterei

Parameter	1	2	3	4
d	50.52	47.89	54.71	51.80
θ	53.63	51.05	52.92	–
σ	51.91	51.55	50.74	50.16
t	44.43	55.34	54.87	–

Table 3 Average values η
3. táblázat Átlagértékek η

The mullite was synthesized at normal pressure varying such input parameters as particle size, heating rate, holding temperature and impurities concentration (which will correspond to the orthogonal array $4^2 \times 3^2 = 144$). The parameters values are presented in *Table 2*, η average values calculated by the ANOVA method – in *Table 3*.

Fig. 3 shows $S/N=\eta$ deviation from its average value. The results of the application of the ANOVA method for data processing are given in *Table 4*.

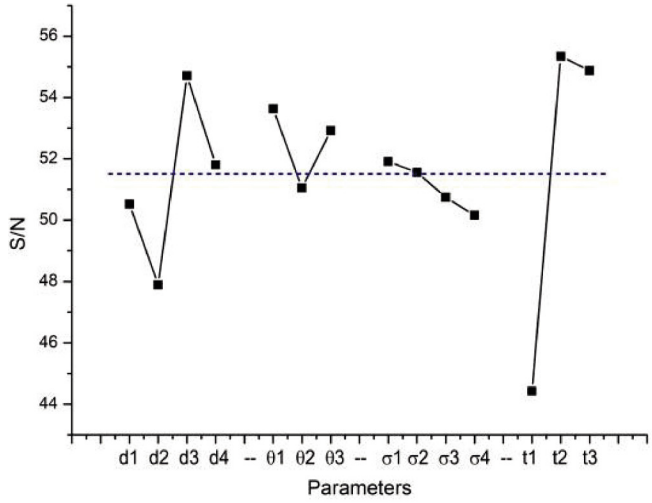

Fig. 3 S/N=η deviation from average value (dashed line)
3. ábra S/N=η eltérés az átlagértéktől (szaggatott vonal)

Parameter	Number of degrees of freedom (df_p)	Sum of squares SS_p	Variance, V	Fisher's criterion F	Parameter influence (%)
d	3	74.45	24.82	0.67	6.48
θ	2	23.90	11.95	0.32	3.12
σ	3	10.13	3.38	0.09	0.88
t	2	685.15	342.58	9.26	89.51
Error	27	296.03	37.00		

Table 4 ANOVA results
4. táblázat ANOVA eredmények

Size of the particles. Reducing the size of the particles results in decreasing temperature of structural transformations (also due to the intensification of diffusion processes during the reaction). Platova and co-authors [34] showed, that in addition to large energy expenses during fragmentation, the regrinding can result in undesirable aggregation of kaolinite particles and, accordingly, to a decrease in the reactionary ability of the surface.

Heating rate. A more uniform heating of the sample, which begins on the surface and gradually spreads throughout the volume of the kaolinite particles, can be achieved with reducing the rate of heat supply (heating rate).

Influence of impurities. The positive impact of impurities is associated with their ability to intensify the process of crystallization-pseudocoagulation structure by accelerating the reaction (for example, with the introduction of group II cations), increasing of mullite yield (TiO_2, LiCl, $MgCO_3$, LiF, etc.) or creating additional crystallization centers (for example, introducing 0.1–1% of the filamentous mullite stimulates crystal formation) [35, 36]. We used impurities of mullite particles as additional crystallization centers.

The formation of the target product – a mullite nanocomposite – has a number of intermediate phases (metakaolinite, pseudomullite) [8]:

$$3(A1_2O_3 \cdot 2SiO_2 \cdot 2H_2O) \Rightarrow 3A1_2O_3 \cdot 2SiO_2 + 4SiO_2 + 6H_2O \quad (3)$$
kaolinite *mullite* *cristobalite*

The theoretical ratio of phases of mullite and cristobalite formed as a result of this reaction is 63.9% to 36.1%. Loss of this ratio indicates the incompleteness of the crystalline transformation of kaolinite with the formation of only intermediate spinel-like phase and pseudomullite, which cannot be reliably identified using X-ray phase analysis.

The influence of input factors – particle size and heating rate – on the intensity of the XRD-peaks of mullite is visualized on the 2D contour plots (*Fig. 4(a)*). *Fig. 4(b)* shows dependence of the content of the mullite phase in the samples on the size of the particles and the heating rate. A comparison of the above contour plots shows that the areas of the greatest intensity of the peaks of the mullite (red region, *Fig. 4(a)*) and the content of the mullite phase in the synthesized sample closest to the theoretical value (blue area, *Fig. 4(b)*) practically coincide. The optimal result is achieved with the size of the particles –0.071+0.1 mm and heating rate 12 deg/min.

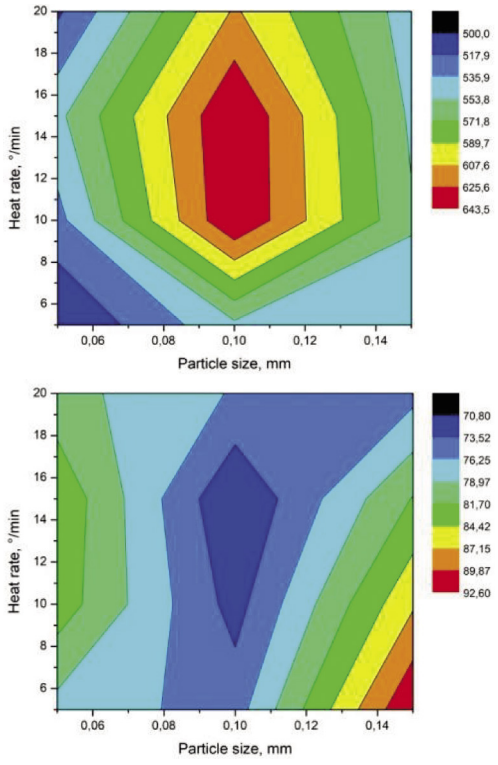

Fig. 4 *2D contour plots of the dependence of the intensity of mullite peaks (a) and content of the mullite phase (b) on the size of the particles and the heating rate. Holding temperature 1150 °C*

4. ábra *2D kontúrdiagramok a mullitcsúcsok intenzitásának (a) és a mullitfázis tartalmának (b) függéséről a részecskék méretétől és a fűtési sebességtől. Tartási hőmérséklet 1150 °C*

The synthesis of mullite nanocomposite from kaolinite in the framework of the optimal protocol was tested (the impurities concentration was 0.5 wt.% corresponding to the point in *Fig. 3*, which is the closest to the average value η). The obtained values of the intensity of the mullite peak (at $2\theta = 40.85°$) at different holding temperatures lie higher than the values measured earlier (the size of the particles +0.1 mm and the heating rate of 10 deg/min, without the introduction of additional crystallization centers), which confirms the formation of the mullite phase at lower temperatures (*Fig. 5*). Taking into account the calculated values (*Table 4*), the proportionality coefficients were calculated: $k_1 = 1.756$, $k_2 = 6.226$, $k_3 = 12.931$.

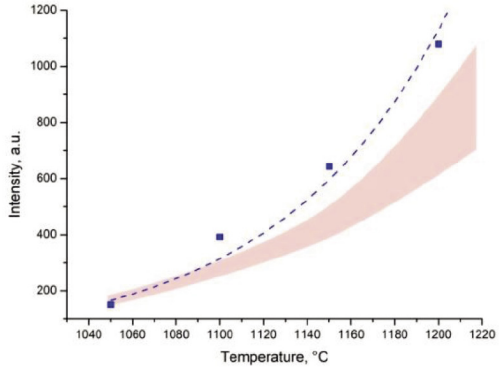

Fig. 5 *Dependence of the intensity of mullite peaks on the temperature of the experiment (dashed curve) with particle sizes –0.071+0.1 mm and a heating rate 12 deg/min. The pink area – values of intensity of mullite peaks in the initial experiments (see Table 2)*

5. ábra *A mullitcsúcsok intenzitásának függése a kísérlet hőmérsékletétől (szaggatott görbe) -0,071+0,1 mm-es részecskeméret és 12 fok/perc fűtési sebesség mellett. A rózsaszín terület - a mullitcsúcsok intenzitásának értékei a kezdeti kísérletekben (lásd a 2. táblázatot)*

The analysis of SEM images confirmed that the optimal protocol is achieved with the sizes of the initial kaolinite particles –0.071+0.05 and –0.1+0.071 mm and temperatures 1150 and 1200 °C, which is consistent with the result obtained above using the Taguchi method and analysis of variance (ANOVA).

Fig. 6 shows the change in the structure of the material under study during heat treatment, depending on the particle size. As the treatment temperature increases, kaolinite grains recrystallize to form larger subindividuals. In addition, elongated pseudomullite crystals appear. At temperatures of 1150 and 1200 °C, the main volume of the samples is compacted; also, at these temperatures, the formation of secondary mullite is typical. It should be noted that –0.05 mm kaolinite fraction is characterized by the formation of subaggregates at lower temperatures than larger fractions. This results in inhibition of the processes of structural transformation of the test substance.

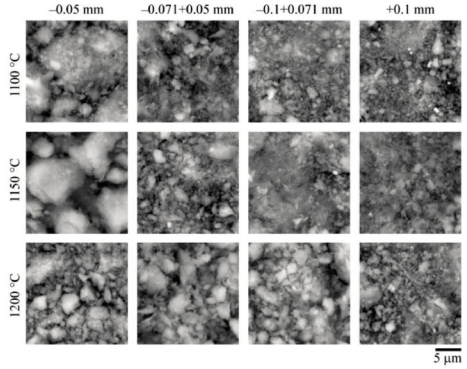

Fig. 6 *Changes in the structure of kaolinite samples with a change in the holding temperature (SEM, back-scattered electrons)*

6. ábra *A kaolinitminták szerkezetének változása a hőmérséklet változásával (SEM, visszaszórt elektronok)*

4. Conclusion

A numerical modeling approach for engineering the quality of a mullite nanocomposite, its physical and structural properties and an optimal synthesis protocol were realized.

Implementing Taguchi experimental design method and analysis of variance (ANOVA) we marked significant parameters in comparison to insignificant ones to obtain nanocomposites with specified characteristics of the ceramic matrix and create the optimal synthesis protocol. On the basis of the obtained experimental data, a mathematical model was re-calculated taking into account the structural and PTX-parameters of the synthesis of mullite from kaolinite.

The 2D contour plots of the intensity of mullite XRD-peaks and content of the mullite phase (mullite content in the synthesized nanocomposite) on the particle size and heating rate showed that the optimal synthesis protocol will be achieved at a particle size of –0.071+0.1 mm and a heating rate of 12 deg/min, which was also confirmed by the experiments. The –0.05 mm fraction of the studied kaolinite was characterized by a higher degree of recrystallization than larger fractions. This resulted in the formation of large subaggregates of kaolinite and, accordingly, to the inhibition of the processes of structural transformation and the formation of the mullite phase.

This paper is a contribution to the development of a technology strategy (process-properties-optimization) for the producing of a mullite nanocomposite with specified technical properties based on structural transformations in the "kaolinite - mullite".

5. Acknowledgements

The work was conducted partly within the framework of the research task [number 1021051101666-2-1.5.1; FUUUU-2022-0059] to develop a technique for estimating the content of aluminosilicate phases on the example of mullite, partly within the framework of RSF project [number 21-47-00019]: study of stability of physicochemical constitution and morphostructural characteristics of mullite.

References

[1] Chakraborty, A.K. (2014) Phase Transformation of Kaolinite Clay. Springer New Delhi. 342 p. http://dx.doi.org/10.1007/978-81-322-1154-9

[2] Cui, K., Zhang, Y., Fu, T. et al. (2020) Toughening Mechanism of Mullite Matrix Composites: A Review. THE Coatings. Vol. 10, pp. 672-696. http://dx.doi.org/10.3390/coatings10070672

[3] Li, S., Li, N. (2005) Influences of composition of starting powders and sintering temperature on the pore size distribution of porous corundum-mullite ceramics. Science of Sintering. Vol. 37, No. 3, pp. 173-180. http://dx.doi.org/10.2298/SOS0503173S

[4] Al-Shantir, O., Trník, A., Csáki, Š. Influence of firing temperature and compacting pressure on density and Young's modulus of electroporcelain. (2018) AIP Conference Proceedings. Vol. 1988, 020001. http://dx.doi.org/10.1063/1.5047595

[5] De Aza, A.H., Turrillas, X., Rodriguez, M.A. et al. (2014) Time-resolved powder neutron diffraction study of the phase transformation sequence of kaolinite to mullite. Journal of the European Ceramic Society. Vol. 34, No. 5, pp. 1409-1421. http://dx.doi.org/10.1016/j.jeurceramsoc.2013.10.034

[6] Egorova, E.Y., Vakalova, T.V., Pogrebenkov, V.M. (2006) Porous ceramics for catalyst carriers based on natural aluminosilicate raw materials. Refractories and technical ceramics. Vol. 7, pp. 30 – 37.

[7] Kacher, E.B., Kremnev, D.V., Mishchenko, A.V. et al. (2006) Research and optimization of the composition and conditions for the synthesis of ceramic products. Scientific and technical bulletin of information technologies, mechanics and optics. Vol. 26, pp. 373-377.

[8] Kotova, O.B., Ustyugov, V.A., Sun, S., et al. (2022) Mullite production: phase transformations of kaolinite, thermodynamics of the process. Journal of Mining Institute. Vol. 254, pp. 129-135. http://dx.doi.org/10.31897/PMI.2022.43

[9] Abdullayev, A., Avcioglu, C., Fey, T., et al. (2022) Fabrication and characterization of porous mullite ceramics derived from fluoride-assisted Metakaolin-Al(OH)3 annealing for filtration applications. Open Ceramics. Vol. 9, 100240. http://dx.doi.org/10.1016/j.oceram.2022.100240.

[10] Romero, M., Padilla, I., Contreras, M., et al. (2021) Mullite-Based Ceramics from Mining Waste: A Review. Minerals. Vol. 11, No. 3, pp. 332. https://doi.org/10.3390/min11030332

[11] Vakalova, T.V., Devyashina, L.P., Tokareva, A.Y. (2013) New mineralizing additive for solid-phase synthesis of mullite and sintering of mullite ceramics from oxides. New refractories. Vol. 3, p. 63.

[12] Pavlov, V.F. (1977) Physical and chemical bases of firing of building ceramics. Stroyizdat, Moscow, 240 p.

[13] Yuan, L., Zhenli, L., Yan, Z., et al. (2022) Effect of mullite phase formed in situ on pore structure and properties of high-purity mullite fibrous ceramics. Ceramics International. Vol. 48, No. 3, pp. 3578-3584. https://doi.org/10.1016/j.ceramint.2021.10.136.

[14] Pletnev, P.M., Pogrebenkov, V.M., Vvereshchagin, V.I., et al. (2017) Mullite-corundum materials based on mullite binder, resistant to high-temperature deformations. New refractories. Vol. 11, pp. 36-43.

[15] Teklay, A., Yina, C., Rosendahl, L., et al. (2015) Experimental and modeling study of flash calcination of kaolinite rich clay particles in a gas suspension calciner. Applied Clay Science. Vol. 103, pp. 10–19. https://doi.org/10.1016/j.clay.2014.11.003

[16] Vakalova, T.V., Pogrebenkov, V.M., Shlyaeva, N.P. (2009) Influence of structural and mineralogical features of silica raw materials on phase changes during its heating. New refractories. Vol. 1, pp. 18-22.

[17] Kotova, O.B., Ignatiev, G.V., Shushkov, D.A. et al. (2019) Preparation and Properties of Ceramic Materials from Coal Fly Ash. Minerals: Structure, Properties, Methods of Investigation Springer. Proceedings in Earth and Environmental Sciences. Springer, Cham. P. 100-107. https://doi.org/10.1007/978-3-030-00925-0_16

[18] Tong, L.X., Li, J.H., Liu, F. (2012) Preparation of Mullite Nanocomposites Powders by the Hydrothermal Crystallization Method from Coal Gangue. Key Engineering Materials. Vol. 512-515, pp. 49-53. https://doi.org/10.4028/www.scientific.net/KEM.512-515.49

[19] Alfonso, P., Penedo, L., Garcia-Valles, M., et al. (2022) Thermal behavior of kaolinitic raw materials from San José (Oruro, Bolivia). Journal of Thermal Analysis and Calorimetry. Vol. 147, pp. 5413–5421. https://doi.org/10.1007/s10973-022-11245-3

[20] Iyasara, A., Boston, R.H., Schmidt, W., et al. (2016) Protocols for the Fabrication, Characterization, and Optimization of n-Type Thermoelectric Ceramic Oxides. Chemistry of Materials. Vol. 29, No. 1, pp. 265–280. https://doi.org/10.1021/acs.chemmater.6b03600

[21] Romero, A.R., Elsayed, H., Bernardo, E. (2018) Highly porous mullite ceramics from engineered alkali activated suspensions // Journal of the American Ceramic Society. Vol. 101, pp. 1036-1041. https://doi.org/10.1111/JACE.15327

[22] Shaneva, A.S., Popova, N.A., Koltsova, E.M. (2017) Research and mathematical modeling of the process of obtaining a ceramic composite material SiC-CNT. Advances in Chemistry and Chemical Technology. Vol. 31, No. 8, pp. 42-44.

[23] Marukovich, E.I., Nikolaychik, Y.A. Improving the efficiency of mold coatings by modifying with nanostructured materials: [non-stick coatings]. (2018) Actual problems of strength: monograph [based on the materials of the 60th International scientific conference "Actual problems of strength", 14–18, May, 2018, Vitebsk] : in 2 volumes / National Academy of Sciences of Belarus, Vitebsk State Technological University. edited by V. V. Rubanik. Vitebsk: VSTU. Vol. 2, Ch. 12, pp. 231-253.

[24] Kosenko, N.F., Filatova, N.V., Pimkov, Y.V. Kinetics of Solid-Phase Synthesis of Mullite from Activated Precursors. (2016) Izvestia of Higher

Educational Institutions. Chemistry and chemical technology. Vol. 59, No. 1, pp. 36-38.
[25] Ponaryadov, A.V., Ustyugov, V.A., Kotova, E.L. (2022) Mathematical approach to studying the process of mullite synthesis. Vestnik of geosciences. Vol. 335, No. 11, pp. 48-54. https://doi.org/10.19110/geov.2022.11.6
[26] Hüner, E. (2020) Optimization of axial flux permanent magnet generator by Taguchi experimental method. Bulletin of the Polish Academy of Sciences, Technical Sciences. Vol. 68, No. 3, 133378
[27] Kokcam, A.H., Uygun, Ö., Taskin, M.F., et al. (2018) Modelling Porosity Permeability of Ceramic Tiles using Fuzzy Taguchi Method. Open Chemistry. Vol. 16, No. 1, pp. 1111-1114. https://doi.org/10.1515/chem-2018-0117
[28] Danilkovich, A.V., Turobov, V.I., Sobolev, E.V., et al. (2016) Application of the Taguchi method to study the structure of a peptide ligand in a complex complex. Mathematical Biology and Bioinformatics. Vol. 11, No. 2, pp. 385–393. https://doi.org/10.17537/2016.11.3851
[29] Celik, N., Turgut, E. (2012) Design analysis of an experimental jet impingement study by using Taguchi method. Heat and Mass Transfer. Vol. 48, pp. 1407-1413. https://doi.org/10.1007/S00231-012-0989-7
[30] Chen, H.J., Chang, S.N., Tang, C.W. (2017) Application of the Taguchi Method for Optimizing the Process Parameters of Producing Lightweight Aggregates by Incorporating Tile Grinding Sludge with Reservoir Sediments. Materials. Vol. 10, No. 11, 1294. https://doi.org/10.3390/ma10111294
[31] Bortnikov, N.S., Mineeva, R.M., Novikov, V.N., et al. (2011) Influence of the size effect on the crystal-morphological properties of kaolinite according to electron microscopy and EPR data (Zhuravliny Log deposit, South Urals). Reports of the Russian Academy Sciences. Vol. 439, No. 2, pp. 240-243.
[32] Shehu, Y., Suzi, S.J., Nur Azam, B. et al. (2017) Chemical Composition and Particle Size Analysis of Kaolin. Path of Science. Vol. 3, No. 10, pp. 1001-1004. https://doi.org/10.22178/pos.27-1
[33] Menezes, R.R., Farias, F.F., Oliveira, M.F., et al. (2009) Kaolin processing waste applied in the manufacturing of ceramic tiles and mullite bodies. Waste Management & Research. Vol. 27, No. 1, pp. 78-86. https://doi.org/10.1177/0734242X07085338
[34] Platova, R.A., Argynbaev, T.M., Stafeeva, Z.V. (2012) Influence of dispersity of kaolin from the Zhurnavliny Log deposit on the pozzolanic activity of metakaolin. Building materials. Vol. 2, pp. 75-79.
[35] Yarotskaya, E.G., Fedorov, P.P. (2018) Mullite and its isomorphic substitutions: review. Condensed media and interfaces. Vol. 20, pp. 537-544. https://doi.org/10.17308/kcmf.2018.20/626
[36] Roy, J., Maitra, S. (2015) Mullitization of aluminosilicate diphasic gel in the presence of nickel oxide additive. Journal of Composite Materials. Vol. 49, No. 13, pp. 1579-1588. https://doi.org/10.1177/0021998314536071

Ref.:
Ponaryadov, A. – **Kotova**, O. – **Kotova**, E.: *Ceramic nanocomposites: control of structural and PTX parameters of the synthesis of mullite from kaolinite using Taguchi experimental design*
Építőanyag – Journal of Silicate Based and Composite Materials, Vol. 75, No. 4 (2023), 148–153. p.
https://doi.org/10.14382/epitoanyag-jsbcm.2023.21